Catal Lett (2009) 127:270–276
DOI 10.1007/s10562-008-9640-0

Catalytic Removal of Toluene over Co_3O_4–CeO_2 Mixed Oxide Catalysts: Comparison with Pt/Al_2O_3

**L. F. Liotta · M. Ousmane · G. Di Carlo ·
G. Pantaleo · G. Deganello · A. Boreave ·
A. Giroir-Fendler**

Received: 16 July 2008 / Accepted: 2 September 2008 / Published online: 7 October 2008

Abstract The catalytic oxidation of toluene, chosen as VOC probe molecule, was investigated over Co_3O_4, CeO_2 and over Co_3O_4–CeO_2 mixed oxides and compared with the catalytic behavior of a conventional Pt(1 wt%)/Al_2O_3 catalyst. Complete toluene oxidation to carbon dioxide and water was achieved over all the investigated systems at temperatures below 500 °C. The most efficient catalyst, Co_3O_4(30 wt%)–CeO_2(70 wt%), showed full toluene conversion at 275 °C, comparing favorably with Pt/Al_2O_3 (100% toluene conversion at 225 °C).

Keywords VOC Combustion · Toluene total oxidation · Co_3O_4–CeO_2 catalysts · Long-term activity test · Pt–Al_2O_3 catalyst

1 Introduction

Catalytic oxidation of organic compounds is one possibility for limiting VOCs emissions since the reaction operates at temperatures much lower than those required for thermal incineration. The advantage of low oxidation temperature is the reduction of fuel consumption, particularly for large volumes of diluted VOC polluted air. Noble metal catalysts present higher activity than metal oxides, but their manufacturing cost is high. Therefore, efforts have been done to develop transition metal oxides with high catalytic activity. Among them, perovskites, manganese and cobalt oxides have received considerable attention for catalytic oxidation of VOCs [1–6]. The presence of ceria-based oxides as supports for perovskites can further improve the specific activity, increasing the dispersion of the perovskite phase and enhancing the oxygen mobility [7, 8]. The high VOCs oxidation activity of Co_3O_4 on Y_2O_3 doped ZrO_2, prepared in presence of ethylenediamine, was ascribed to the improved dispersion of cobalt oxide along with to the reducibility of cobalt species, at low-temperature, promoted by yttrium [5, 6]. Doping ZrO_2 by Y_2O_3 induces formation of anionic vacancies, which key role was claimed in propene and toluene oxidation [9].

On the other hand, pure ceria was the most active catalyst for toluene oxidation, between a series of ceria–zirconia mixed oxides, since the combustion of toluene was essentially controlled by the presence of surface oxygen species which facilitate the C–H bond activation [10].

Recently, our group reported for a series of Co_3O_4–CeO_2 mixed oxides high effectiveness and stable catalytic performances for methane and propene oxidation, highlighting a different role of surface and bulk oxygen in the two reactions [11, 12]. As methane oxidation doesnot start until 300 °C, at such high-temperature the reaction

---

The work was presented during the conference Catalysis for Society, Krakow, May 11-15, 2008.

L. F. Liotta (✉) · G. Pantaleo · G. Deganello
Istituto per Lo Studio dei Materiali Nanostrutturati (ISMN)-CNR, via Ugo La Malfa, 153, Palermo 90146, Italy
e-mail: liotta@pa.ismn.cnr.it

M. Ousmane · G. Di Carlo · G. Deganello
Dipartimento di Chimica Inorganica e Analitica “Stanislao Cannizzaro”, Università di Palermo, Viale delle Scienze, Parco d'Orleans II Pad. 17, Palermo 90128, Italy

M. Ousmane · A. Boreave · A. Giroir-Fendler
Université de Lyon, Lyon 69003, France

M. Ousmane · A. Boreave · A. Giroir-Fendler
Université Lyon 1, Villeurbanne 69622, France

M. Ousmane · A. Boreave · A. Giroir-Fendler
CNRS, UMR 5256, IRCELYON, 2 Avenue Albert Einstein, Villeurbanne 69622, France

involves lattice oxygen, while propene oxidation, occurring at lower temperature, is essentially controlled by surface electrophilic oxygen species.

On these bases, in the present work we considered worthwhile to investigate over the Co_3O_4–CeO_2 systems the oxidation of toluene, present in the industrial and automotive emissions, a polluting VOC molecule because of its high photochemical ozone creativity potential (POCP) [13]. The catalysts in question were the same samples used for propene oxidation [12]. The influence of surface and bulk oxygen mobility in the toluene oxidation properties was studied. Moreover, in order to assess the effect of surface oxygen species on the activity, two ceria samples with different surface area, 37 and 13 m^2/g, respectively, were tested. To evaluate the catalytic performances of Co_3O_4–CeO_2 mixed oxides catalyst, a conventional platinum catalyst was also studied. The attention was focused on the maintenance of the catalyst stability. To this aim, three consecutive heating–cooling cycles over selected samples were performed. Moreover, long-term activity tests for 45 h at 200 °C and at 400 °C over the most active catalyst were also carried out. He-TPD and O_2-TPO experiments were carried out over the used catalyst in order to detect if coke formation occurs.

2 Experimental

Co_3O_4, CeO_2 and a series of Co_3O_4–CeO_2 catalysts with increasing Co_3O_4 loading, i.e., 5, 15, 30, 50 and 70%, were prepared by co-precipitation method with sodium carbonate solution (1 M) and calcined at 650 °C for 5 h, as described elsewhere [12]. The so obtained materials (*as prepared samples*) were labeled as Co*x*Ce (where *x* refers to the Co_3O_4 weight content). A portion of ceria oxide calcined at 650 °C was further treated at 750 °C for 5 h and labeled as CeO_2 750.

The reference Pt(1 wt%)/Al_2O_3 catalyst was prepared from commercial γ-Al_2O_3 (Rhodia-SPH569) by impregnation method with a solution of $Pt(NH_3)_4Cl_2$ (Pfaltz and Bauer) [14]. After drying overnight, the sample was calcined at 500 °C for 2 h and reduced under flowing hydrogen (10 L/h) at 300 °C for 2 h.

Specific surface area (SSA) measurements were performed with a Sorptomatic 1900 Carlo Erba instrument, by physical adsorption of N_2 at the liquid nitrogen temperature, using the BET equation.

X-ray diffraction patterns were recorded with a D 5005 X-ray Diffractometer (SIEMENS) using Cu Kα radiation coupled with a graphite monochromator. A divergence slit of 0.2°, a proportional counter and 0.03° step sizes in 2θ were used. The instrumental contribution and the resolution function for the instrumental broadening were calculated using lanthanum boride (NIST). The assignment of crystalline phases was based on ICSD data base (Co_3O_4 No. 2,4210, CeO_2 No. 2,8785) [15]. From the line broadening of the main reflection peaks (line 311 for Co_3O_4 and line 111 for CeO_2), particle sizes (*d*) of the crystalline phases were calculated. The estimated error was ±10%.

Temperature Programmed Reduction (TPR) experiments were carried out with a Micromeritics Autochem 2910 apparatus equipped with a thermal conductivity detector (TCD). The reducing gas, a mixture of 5 vol% H_2 in Ar, at a flow rate of 1.8 L/h, was flowed over the pre-oxidized sample, by increasing the temperature from room temperature to 1,000 °C at a rate of 10 °C/min. The amount of sample used for pure Co_3O_4 (0.012 g) was properly increased for the mixed oxides, depending on the Co_3O_4 content. For pure CeO_2 an amount of sample equal to 0.1 g was used.

The catalytic activity measurements were carried out in a tubular fixed-bed reactor, under a reactive mixture containing 1,000 ppm of C_7H_8 and 9% O_2 in He. The concentration of reactant gases was adjusted by a Calibrage PUL010 apparatus constituted of a saturator (for toluene) and two mass flow controllers (BROOKS). The total gas flow rate was 7.2 L/h and the amount of catalyst 0.2 g, equivalent to a weight hourly space velocity (WHSV) of 36 L/g h. The temperature was increased from room temperature to 500 °C (rate 1.3 °C/min). Reactants and products were analyzed by gas chromatography (CPG, PERKIN ELMER Clarus 500) equipped with FID and TCD as well as using IR analyzer (ROSEMOUNT Binos 1004). The only reaction products were CO_2 and H_2O and the carbon balance was close to ±5%. In order to monitor possible catalyst deactivation processes, over selected samples three reaction runs (heating–cooling cycle) from room temperature up to 500 °C were recorded consecutively. The difference between the cycles did not exceed 20 °C, except for pure ceria showing a pronounced deactivation after the first catalytic run. Therefore, to compare the catalytic performance, the first run was considered.

Long-term activity tests (at constant WHSV equal to 36 L/g h) were performed over a selected sample, Co30Ce, at two different temperatures, 200 °C and 400 °C for 45 h.

He-TPD and O_2-TPO experiments were performed using the same apparatus as for catalytic tests. The catalyst, after long-term activity tests, was cooled down to r.t. under the reaction mixture, and divided in two parts (0.1 g each portion); then TPD and TPO experiments carried out under He or 5% O_2/He (3.6 L/h) by increasing the temperature up to 900 °C (rate 10 °C/min). The reactor outflow gases were analyzed on line by mass quadrupole (Thermostar^{TM}, Balzers).

3 Results and Discussion

Figure 1 gives the toluene conversion curves versus temperature. In Table 1, the temperatures of 20, 50 and 100% of C_7H_8 conversion are listed. Depending on the catalyst composition, toluene oxidation started at temperature between 200 and 300 °C and full conversion was achieved at temperature $\leq$450 °C. The lowest temperature was observed for pure CeO_2, followed by Co30Ce and, then, by Co_3O_4. For the remaining Co*x*Ce samples the activity increased by increasing the Co_3O_4 weight content.

BET and XRD characterizations of the samples were already reported [12], however, for a prompt view of the textural properties, in Table 2 the specific surface area values along with the mean crystallite diameters for as prepared catalysts were listed. Values referred to the ceria sample calcined at 750 °C were also enclosed. BET surface area measurements showed for Co*x*Ce mixed oxides surface area values ranging between ~20 and 30 m^2/g, while pure oxides, Co_3O_4 and CeO_2 had 11 and 37 m^2/g, respectively. Crystalline features of both, Co_3O_4 spinel and CeO_2 fluorite, were detected by XRD in the Co*x*Ce mixed catalysts, except for Co15Ce and Co5Ce samples not showing clearly visible Co_3O_4 features, probably because of the low cobalt content. In Fig. 2a, b the XRD patterns of some selected samples, as prepared and after three toluene oxidation cycles, are displayed. The catalytic ageing did not affect the samples crystallinity, being the mean particle size values of the used samples close to the fresh ones.

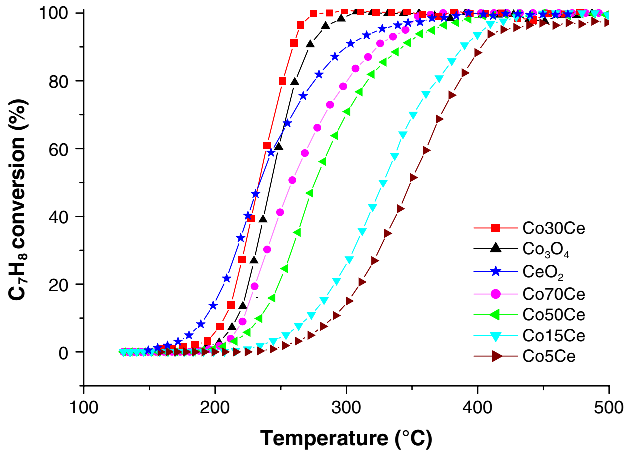

Fig. 1 C_7H_8 conversion (%) over Co_3O_4, CeO_2 and Co*x*Ce catalysts as a function of reaction temperature (°C), during the first catalytic run from room temperature up to 500 °C

Table 1 Temperatures (°C) of 20, 50 and 100% of C_7H_8 conversion during the first catalytic run from room temperature up to 500 °C

Sample	T_{20} (°C)	T_{50} (°C)	T_{100} (°C)
Co_3O_4	225	242	305
Co70Ce	231	257	355
Co50Ce	248	275	393
Co30Ce	216	233	275
Co15Ce	291	328	419
Co5Ce	311	348	450
CeO_2	206	233	365
CeO_2 750	338	382	480
Pt(1%)/Al_2O_3	161	180	225

Table 2 Textural properties of as prepared Co*x*Ce samples

Sample	SSA (m^2/g)	$d_{Co_3O_4}$ (nm)	d_{CeO_2}
Co_3O_4	11	72	
Co70Ce	21	43	22
Co50Ce	22	31	21
Co30Ce	33	14	15
Co15Ce	24	ND	25
Co5Ce	29	ND	28
CeO_2	37	–	23
$CeO_2$750	13	–	39

ND Not detectable

As previously remarked [11, 12], the progressive addition of ceria to cobalt oxide, from Co_3O_4 up to Co5Ce, favored dispersion of Co_3O_4 crystallites and increased the surface area (Table 2). Moreover, it is worth noting that Co30Ce sample exhibited unexpected improved textural properties. This apparently odd behavior was consistent with investigations performed over a previous synthesized Co30Ce sample [11] showing that due to the peculiar composition (Co/Ce atomic ratio = 1) the best interaction between the two oxides, Co_3O_4 and CeO_2, was favored. The achievement of cobalt oxide finely dispersed and strongly interacting with ceria has been also reported by other authors for certain Co_3O_4–CeO_2 systems, appropriately synthesized, and has been claimed that these CoO*x* species mainly contribute to the catalytic activity [16, 17].

In order to check the reproducibility of the reduction properties of the new series of Co*x*Ce systems, characterizations TPR of selected catalysts, as prepared and after three consecutive toluene oxidation cycles, were performed in the present paper. In Fig. 3, the reduction profiles are displayed. Among the Co*x*Ce samples investigated, the reducibility was greatly increased in the sample Co30Ce that starts the reduction at 200 °C with an intense peak centered at 250 °C, which hydrogen uptake (29 mL/g) well accounts for the reduction of Co_3O_4 to CoO. A further reduction occurred between 300 and 500 °C, with hydrogen consumption of 114 mL/g. The broadened shape of this peak suggests that there are different species reducing in the same range of temperature. According to our previous results [11], the hydrogen uptake accounts for the

Fig. 2 XRD patterns of selected samples. Panel (a) refers to fresh catalysts; panel (b) to the catalysts after three catalytic cycles

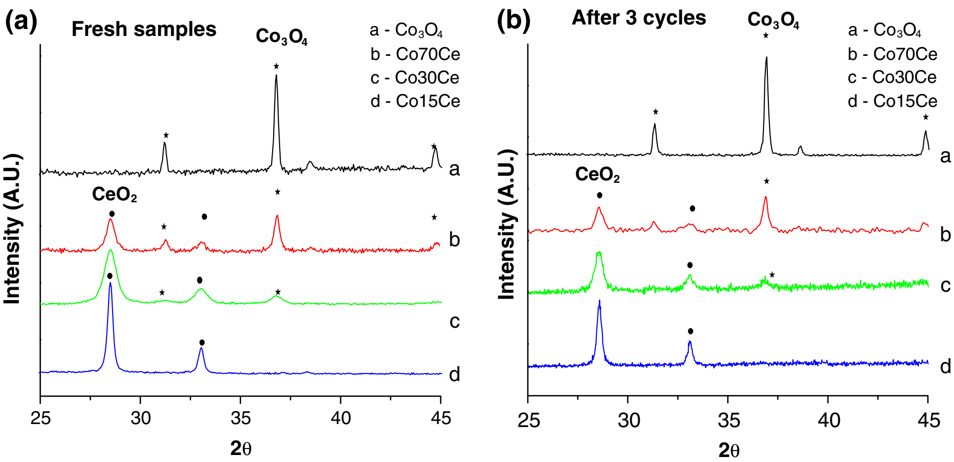

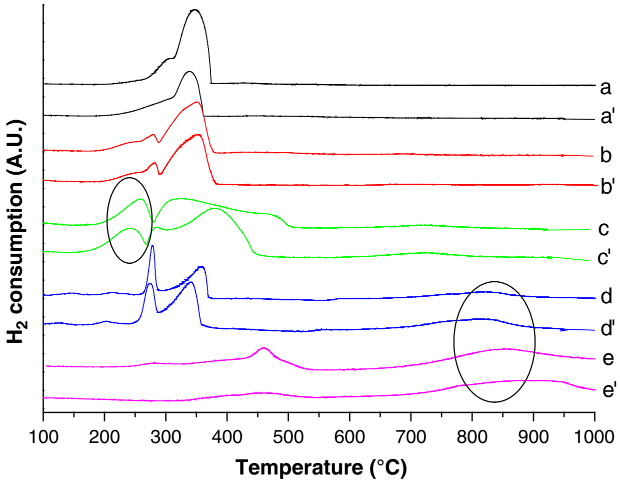

Fig. 3 H_2-TPR profiles of selected Co*x*Ce samples as fresh and after three catalytic cycles: (a) Co_3O_4, (b) Co70Ce, (c) Co30Ce, (d) Co15Ce, (e) CeO_2. The a′, b′ characters refer to the used catalysts

Table 3 Specific reaction rates (μmol C_7H_8 s^{-1} $g^{-1}_{catalyst}$) calculated at 200 and 250 °C over Co_3O_4, CeO_2 and Co*x*Ce catalysts, during the first catalytic run

Sample	*r* (μmol C_7H_8 s^{-1} $g^{-1}_{catalyst}$)[a]	*r* (μmol C_7H_8 s^{-1} $g^{-1}_{catalyst}$)[b]
Co_3O_4	0.012	0.270
Co70Ce	0.008	0.182
Co50Ce	0.002	0.107
Co30Ce	0.019	0.403
Co15Ce	0	0.022
Co5Ce	0	0.008
CeO_2	0.061	0.301

[a] Calculated at 200 °C

[b] Calculated at 250 °C

reduction of CoO to Co metal along with the reduction of surface and bulk ceria. It is worth noting that the absence of the high-temperature peak, at around 800 °C, typical of bulk ceria reduction would confirm a mutual interaction cobalt–cerium oxides responsible of enhanced reduction properties. Similarly to Co30Ce, the TPR curves of Co_3O_4 and of the other Co*x*Ce oxides showed at around 300–350 °C two main reduction peaks, which temperature and relative intensities, however, depends on the sample composition. In the curve of Co15Ce, an additional signal around 800 °C is visible due to the reduction of ceria bulk not in contact with cobalt. For pure ceria, the reduction profile showed a high-temperature peak (at 840 °C) due to bulk oxygen species, while the low-temperature peak (at 460 °C) was attributed to the reduction of surface oxygen species [18].

It is important to observe that no appreciable influence of the ageing, upon three catalytic cycles, was observed on the reduction properties of Co*x*Ce. On the contrary, it is worth noting that for pure ceria the low-temperature reduction peak almost disappeared in the aged sample, suggesting decreased surface oxygen mobility.

In conclusion, TPR experiments evidenced, accordingly to our previous results [11], that the addition of ceria to Co_3O_4 promotes the reduction of Co^{3+} to Co^{2+} at a lower temperature than bare Co_3O_4, the catalyst reducibility following the order: Co30Ce > Co15Ce > Co_3O_4 ≫ CeO_2.

In order to have a more complete picture of the factors influencing the activity, the catalytic results, expressed as specific reaction rates (μmol C_7H_8 s^{-1} $g^{-1}_{catalyst}$), were calculated at 200 and at 250 °C (Table 3), assuming a first order reaction with respect to toluene and pseudo-zero order with respect to oxygen [8]. Among the catalysts, at 200 °C, CeO_2 was much better performing than Co30Ce and Co_3O_4. At slightly higher temperature, 250 °C, however, Co30Ce became more active than CeO_2 and Co_3O_4, the latter one being slightly less active than ceria. For the remaining Co*x*Ce samples, the activity decreased by decreasing the Co_3O_4 weight content.

Table 4 Activation energy (E_{act}) and pre-exponential factor A relative to toluene oxidation

Sample	E_{act} (kJ/mol)	ln A
Co_3O_4	58	15
Co70Ce	68	17
Co50Ce	73	18
Co30Ce	57	15
Co15Ce	78	18
Co5Ce	80	18
CeO_2	62	16
CeO_2 750	87	19

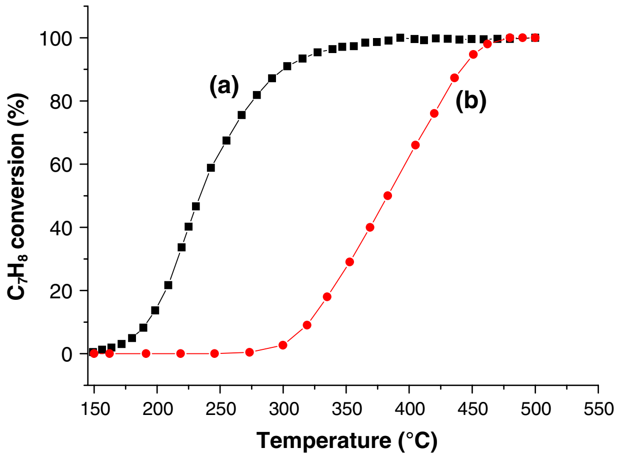

Fig. 4 C_7H_8 conversion (%) over two ceria samples calcined at: (a) 650 and (b) at 750 °C as a function of reaction temperature (°C)

For all catalysts, the corresponding Arrhenius plots were linear for conversion values between 10 and 90%, excluding the occurrence of diffusional effects. In Table 4, the apparent activation energies E_{act} along with the pre-exponential factor A of the Arrhenius equation, $k = A \exp(-E_{act}/RT)$, were listed. E_{act} values as small as 57–62 kJ/mol were obtained for the most active samples, Co30Ce, Co_3O_4 and CeO_2, while E_{act} of 78–80 kJ/mol were obtained for Co15Ce and Co5Ce. The values for the other Co*x*Ce samples were between the above two values. Variations of the pre-exponential factors reflect changes of the active site ensemble. The calculated activation energies are comparable with values previously reported for toluene oxidation over perovskites [8].

On the basis of data so far reported (Fig. 1 and Table 3), pure CeO_2 was the most active sample at 200 °C, however, at $T \geq 250$ °C the activity changed as Co30Ce > CeO_2 > Co_3O_4. An explanation of the observed catalytic behavior is discussed. Ceria is well known for its oxygen storage capacity [18] and the role of surface oxygen vacancies in activating toluene oxidation reaction was clearly demonstrated [10]. Moreover, recently, we have reported that electrophilic oxygen species, transiently produced by oxygen adsorption on the surface reduced defects of ceria [19], governed the oxidation activity of propene [12].

To get further insight in the role of surface oxygen species in the toluene oxidation, the catalytic behavior of two ceria samples different in surface area values was compared. Being oxygen surface properties directly related to the surface area [18], an effect on the catalytic performances should occur if such properties are really determining the activity.

A portion of ceria calcined at 650 °C, having surface area of 37 m^2/g, was further treated at 750 °C for 5 h in order to decrease the specific surface area (BET = 13 m^2/g). At the same time, a sintering of ceria crystallites occurred (Table 2). The toluene conversion curves over the two ceria samples are displayed in Fig. 4. The sample calcined at 750 °C was dramatically less active and the temperature of 50% toluene conversion was shifted of ~150 °C to higher values (see Table 1). The deactivation of CeO_2 750 sample is in good agreement with the lowered oxidation performance observed for fresh ceria after three consecutive catalytic runs (heating–cooling cycle). Furthermore, the TPR profiles of fresh and aged ceria (Fig. 3, curves e, e′) further confirm the diminished surface oxygen mobility of sintered ceria, which accounts for a lower oxidation activity.

With respect to the oxidation activity of Co_3O_4-based catalysts, it is generally accepted that oxygens octahedrally coordinated around Co^{3+} ions are highly active species in hydrocarbons oxidations [20, 21]. Moreover, Co^{2+} ions in tetrahedral and Co^{3+} ions in octahedral coordination positions should be active centers for adsorption of oxygen and hydrocarbons, respectively, [22–24]. On the other hand, oxygen bulk mobility seems to play also an important role in the catalytic oxidation over reducible metal oxides [25]. Accordingly, Co*x*Ce mixed oxides are suitable catalysts for methane oxidation and a clear correlation between activity and redox properties was found [11]. Furthermore, we have demonstrated the role of surface oxygen vacancies and bulk oxygen mobility in propene oxidation over Co*x*Ce oxides [12]. On the contrary, in the case of ceria the propene oxidation involved only oxygen species filling surface vacancies [12], accordingly to the poor bulk oxygen mobility [26].

To summarize, on the basis of the present toluene oxidation data, for Co*x*Ce systems the active species seems to be the Co_3O_4 phase, which activity, textural and reduction properties were strongly modified by interaction with ceria. Accordingly, the peculiar behavior of Co30Ce sample was justified by an improvement of the dispersion as well as of the reduction properties of the Co_3O_4 species. Indeed, the toluene oxidation performances of Co*x*Ce catalysts well-correlated with the TPR results (Fig. 3), namely the lower

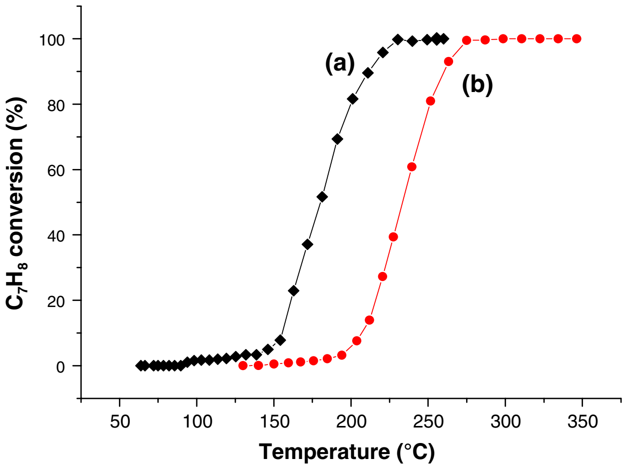

Fig. 5 C_7H_8 conversion (%) over: (a) Pt(1 wt%)/Al_2O_3 and (b) Co30Ce as a function of reaction temperature (°C). (Note that the C_7H_8 conversion curve over Co30Ce is the same one as plotted in Fig. 1 and here was repeated to make an easier comparison with Pt(1 wt%)/Al_2O_3)

reduction temperature corresponded to the higher activity, in agreement with literature results [5, 6, 9].

In order to evaluate the catalytic performances of the most active Co30Ce catalyst, a conventional platinum catalyst was also studied (Fig. 5). The mixed oxide compares well with the reference, being slightly less active than the Pt alumina (only 50 °C at higher temperatures, Table 1).

Finally, as one of the most important properties of a catalyst is the maintenance of long-term activity, we carried out over Co30Ce a lifetime test by feeding the reaction mixture at 200 and 400 °C for 45 h on stream (see Fig. 6a, b). No significant deactivation was observed at the two selected temperatures, being the toluene conversion stable at 7 and 100% (±2%) for the whole test. The slight variations in toluene conversion well-agree with any accumulation of water and/or carbon dioxide on the catalyst surface, which easily desorbs under the reaction stream.

After life-tests at 200 and 400 °C, the sample showed a decreased surface from 33 m^2/g to 20 and to 16 m^2/g, respectively, while no appreciable sintering of Co_3O_4 and CeO_2 crystallites occurred. Co_3O_4 crystallite sizes around 25 nm were detected by XRD.

The stable catalytic performance of Co30Ce after 45 h under reaction stream, in spite of a diminished surface are due to the thermal ageing may confirm the involvement of lattice oxygen in the toluene oxidation.

No coke deposition was evidenced, as demonstrated by He-TPD and TPO experiments carried out over two portions of the used catalyst. Some CO_2 evolution occurred

Fig. 6 Long-term activity test over Co30Ce for 45 h at: (a) 200 °C; (b) 400 °C

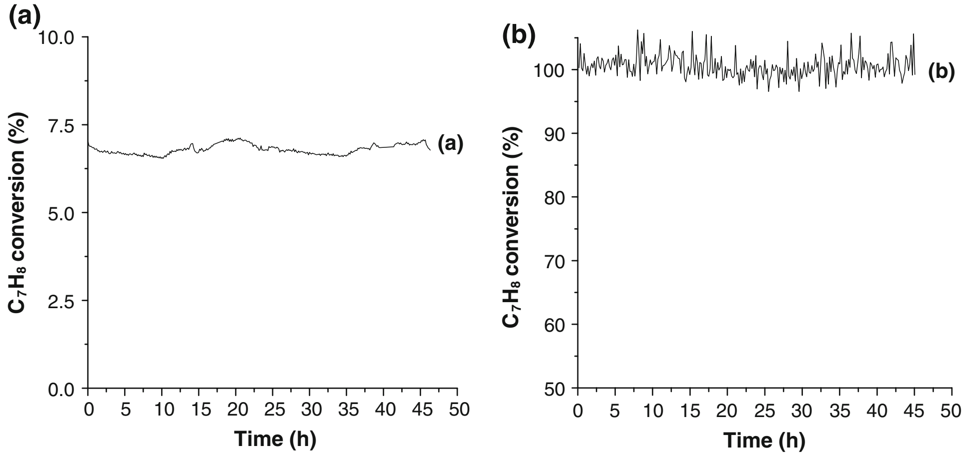

Fig. 7 QMS signals recorded after a long-term activity test (at 400 °C for 45 h) over Co30Ce: (a) He-TPD experiment; (b) TPO (5%O_2/He) experiment

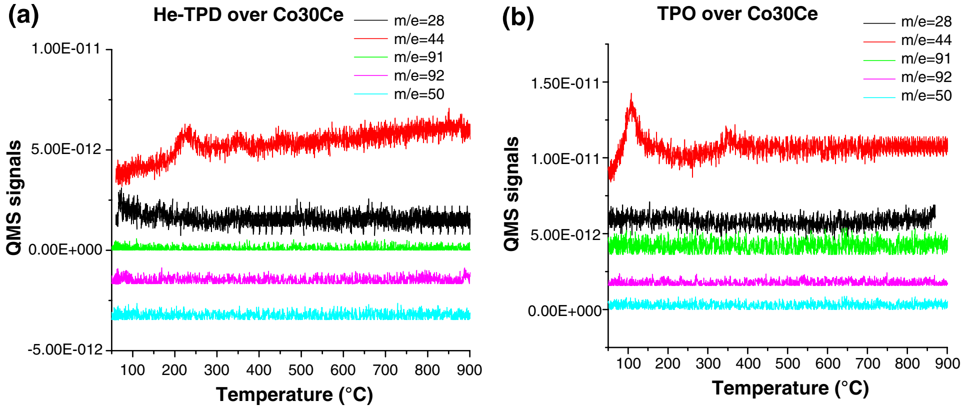

with peaks at around 220 °C in He-TPD and at 110 °C in TPO curves, respectively (Fig. 7a, b). No other signals at $m/e = 91, 92, 50$ attributable to residual toluene fragments were detected.

4 Conclusions

The catalytic oxidation of toluene was studied over pure Co_3O_4 and CeO_2 oxides and over a series of Co_3O_4–CeO_2 mixed oxides and compared with a conventional catalyst Pt(1wt%)/Al_2O_3. Complete toluene oxidation to carbon dioxide and water was achieved over all the investigated catalysts at temperatures below 500 °C. The catalyst stability was tested over selected samples performing three reaction runs (heating–cooling cycle) from room temperature up to 500 °C. It was found that Co*x*Ce catalysts maintained a good stability, while pure ceria showed a pronounced deactivation after the first catalytic run. Moreover, a portion of ceria sample calcined at 750 °C was significantly less active than the fresh sample.

The participation of surface oxygen species and high mobile bulk oxygen were the factors determining the activity of Co_3O_4 and Co*x*Ce samples. On the contrary, toluene oxidation on ceria was governed only by the amount of available surface oxygen, according to catalytic and TPR results.

The most efficient catalyst Co30Ce, characterized by Co/Ce atomic ratio equal to 1, reached full toluene conversion at 275 °C, which was only 50 °C higher than the temperature of 100% conversion over Pt alumina. As an important property, the Co30Ce catalyst exhibited stable toluene oxidation activity during lifetime tests, running for 45 h at 200 and 400 °C.

These results demonstrated that the Co30Ce mixed oxide is a good candidate for VOCs abatement confirming that transition metal oxides can be used for the combustion of VOCs at low-temperature.

Acknowledgment Bilateral Project CNR-CNRS (2006–2007) is gratefully acknowledged for financial support.

References

1. Alifanti M, Florea M, Somacescu S, Pârvulescu VI (2005) Appl Catal B: Environ 60:33
2. Lamaita L, Peluso MA, Sambeth JE, Thomas HJ (2005) Appl Catal B: Environ 61:114
3. Ataloglou T, Vakros J, Bourikas K, Fountzoula C, Kordulis C, Lycourghiotis A (2005) Appl Catal B: Environ 57:299
4. Wyrwalski F, Lamonier J-F, Perez-Zurita MJ, Siffert S, Aboukaïs A (2006) Catal Lett 108:87
5. Wyrwalski F, Lamonier J-F, Siffert S, Aboukaïs A (2007) Appl Catal B: Environ 70:393
6. Wyrwalski F, Lamonier J-F, Siffert S, Gengembre L, Aboukaïs A (2007) Catal Today 119:332
7. Alifanti M, Florea M, Cortes-Corberan V, Endruschat U, Delmon B, Pârvulescu VI (2006) Catal Today 112:169
8. Alifanti M, Florea M, Pârvulescu VI (2007) Appl Catal B: Environ 70:400
9. Labaki M, Siffert S, Lamonier J-F, Zhilinskaya EA, Aboukaïs A (2003) Appl Catal B: Environ 43:261
10. de Rivas B, Gutiérrez-Ortiz JI, López-Fonseca R, González-Velasco JR (2006) Appl Catal A: Gen 314:54
11. Liotta LF, Di Carlo G, Pantaleo G, Venezia AM, Deganello G (2006) Appl Catal B: Environ 66:217
12. Liotta LF, Ousmane M, Di Carlo G, Pantaleo G, Deganello G, Marcì G, Retailleau L, Giroir-Fendler A (2008) Appl Catal A: Gen 347:81
13. Fontane H, Veillerot M, Gallo JC, Guillermo R (1999) In: Proceedings of the 8th international symposium on transport and air pollution, Graz, 1999
14. Benard S, Retailleau L, Gaillard F, Vernoux P, Giroir-Fendler A (2005) Appl Catal B: Environ 55:11
15. Inorganic Crystal Structure Data Base (ICSD), National Institute of Standards and Technology (NIST), release 2004/2
16. Kang M, Song MW, Lee CH (2003) Appl Catal A: Gen 251:143
17. Luo J-Y, Meng M, Li X, Li X-G, Zha Y-Q, Hu T-D, Xie Y-N, Zhang J (2008) J Catal 254:310
18. Trovarelli A (2002) Catalysis by ceria and related materials. Imperial College, London
19. Binet C, Daturi M, Lavalley J-C (1999) Catal Today 50:207
20. Golodets GI (1983) Heterogeneous catalytic reactions involving molecular oxygen, studies in surface science and catalysis, vol 15. Elsevier, Amsterdam
21. Bielanski A, Haber J (1991) Oxygen in catalysis. Marcel Dekker, New York
22. Łojewska J, Kołodziej A, Żak J, Stoch J (2005) Catal Today 105:655
23. Drago RS, Jurczyk K, Singh DJ, Young V (1995) Appl Catal B: Environ 6:155
24. Milt VG, Ulla MA, Lombardo EA (2000) Catal Lett 65:67
25. Moro-oka Y, Ueda W, Lee K-H (2003) J Mol Catal A: Chem 199:139
26. Kašpar J, Fornasiero P, Graziani M (1999) Catal Today 50:285